Moment Capacity of Steel Beams with Hollow Flanges

Youssef Saad Fathi, Ahmed Hassan Yousef, Ahmed Abdelmageed Matloub, Mona Mahmoud Fawzy

Abstract— Hollow flange beams (HFB) are introduced in steel construction because of their torsional stiffness that can resist the lateral torsional buckling. HFB enhances the moment capacity compared to the common I-beams with plated flange. This paper presents moment capacity of HFB using FEM to check the applicability of AISC code. Compact, noncompact and slender sections are considered in the study. The results indicates that web slenderness ratio affects the moment capacity more than the flange slenderness ratio. Conservative AISC capacity is noticed for beams with slender web but on contrary for noncompact web. A modified design equations in AISC to predict the moment capacity of HFB is introduced showing close results with FEM.

Index Terms— hollow flange, moment capacity, AISC, FEM.

1 Introduction

Steel I-section plate girders (IPGs), obtained by the assemblage of flange and web plate elements, are currently basic elements in modern construction. Their behavior depends on the structural response of the plate elements that are subjected mainly to in-plane loading. Steel design standards normally define the flexural resistance of IPGs based on the consideration of local buckling (LB) and lateral–torsional buckling (LTB) limit states. In general, LB of IPGs is defined as a mode involving deformations of their individual plates without the translation of the intersection lines of the adjacent plate elements. Accordingly, the LB depends on the slenderness ratios of flange and web elements. Conversely, the LTB, which depends upon the unbraced length, is characterized by a rigid-body lateral translation and twist of the cross-section. However, the moment capacity of an IPG failing by LTB is limited to a value less than the moment required to produce significant yielding of their cross-section. On the other hand, it is common fact that IPGs can fail in a manner in which the web distorts into an S shape. This mode of failure is commonly known as the lateral–distortional buckling (LDB). In general, LB of IPGs is defined as a mode in which individual plates are deformed without the junction lines of adjacent plate elements being translated. As a result, the LB is determined by the flange and web element slenderness ratios. The LTB, on the other hand, is characterised by rigid-body lateral translation and twist of the cross-section, which is dependent on the unbraced length. The moment capacity of an IPG failing by LTB, on the other hand, is limited to a value less than the moment required to produce significant cross-section yielding. IPGs, on the other hand, are known to fail in a way that causes the web to distort into an S shape. The lateral–distortional buckling failure mode is a typical name for this type of failure (LDB).

2 Literature Review

The steel I shape is the common section used for beams. The design of beams depends on the section slenderness limit of its flange and web. Also, the unsupported length of the compression flange affects the beam capacity. New profile is introduced using hollow flange instead of plate flange as shown in Figure 1. This section enhances the moment capacity due to its higher flange stiffness. The idea was started with triangle flange [1], then transformed to rectangular flanges in C-profile [2 to 4]. Recently, hollow flange beams (HFB) with deep depth have been introduced to be used in long span beams. These sections consist of hollow tubular section welded to web. Many studies on HFB were performed but the AISC did not introduce equations for this section yet.

HFB was studied in some researches [5 to 7]. A study is performed on HFB with slender web and the results showed higher moment capacity than sections with plate flanges having same area [8]. Euro norm equations were found unconservative. Lateral distortional buckling governed the failure modes. The same models were studied after adding stiffeners to the web to enhance the failure mode [9]. The failure modes become lateral torsional buckling instead of the previous lateral distortional buckling and the moment capacity increased. More studies were conducted on HFB such as moment modification factor [10] and beams subjected to shear [11 & 12].

The aim of this paper is continuing the previous studies on HFB considering different section classifications, in addition of proposing equations for the moment capacity applied to HFB in AISC 360-16 [13]. Finite element modeling is used with ABAQUS software [14].

- *Youssef Saad, Demonstrator, Civil Engineering Department, The Higher Institute of Engineering El-Shorouk, master student at Ain Shams university, Cairo, youssefsaadrizk@gmail.com*
- *Ahmed Hassan, Professor, Structural Engineering Department, Ain Shams university, Cairo, ahmed_aly@eng.asu.edu.eg*
- *Ahmed AbdelMageed, Assistant professor, Structural Engineering at Ain Shams university, Cairo, ahmed.matloub@eng.asu.edu.eg.*
- *Mona Mahmoud, Lecturer, Civil Engineering Department, The Higher Institute of Engineering El-Shorouk elshorouk academy, m.fawzy@sha.edu.eg*

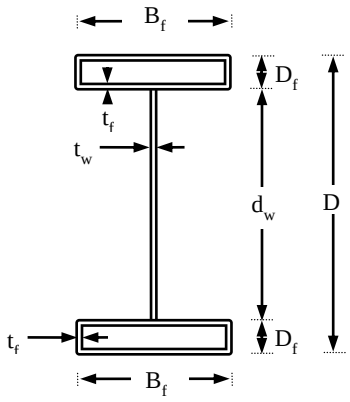

Fig.1: Hollow Flange Beam (HFB)

3 FEM VALIDATION

FEM is used to develop models for HFB and finite element analysis can be used to study the moment capacity. Commercial package ABAQUS is used for the modeling. The methodology is verified with previous experimental work and the accuracy is found good.

The beams are modeled using nonlinear thin shell element having four nodes and reduced integration, so-called S4R. Size of mesh is taken 50 x 50 mm and half beam is modeled as a result of beam symmetry as shown in Figure 2. At support, bottom flange is restrained from Z displacement and the section is restrained from Y displacement and X rotation. Axi-symmetric boundary condition is applied at the symmetry plane at mid-span. Couple opposite normal force is applied to both flanges to produce constant moment along the beam length. For the steel material, nonlinear material is used with bilinear stress-strain and strain hardening curve. The Young's modulus is taken 200,000 MPa and tangent modulus of 2,000 MPa starting at yield stress equal 355 MPa. Buckling analysis is used to perform the initial buckling deformation then the deformed geometry is used in the analysis to take into account the initial imperfection. Combined buckling modes from local buckling and lateral torsional buckling are considered. The initial deformation is adapted to value of plate width / 300 for local buckling and beam length / 1000 of lateral torsional buckling.

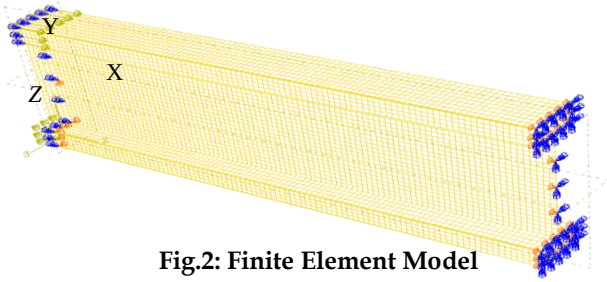

Fig.2: Finite Element Model

Verification with previous experimental works is performed to validate the finite element process and ensure accurate results. Two papers are used in the verification step [15 & 16]. Six specimens are used as presented in Table 1 and the results show good accuracy. The difference between FEM and experiments is less than 10% with an average ratio and standard deviation value of 0.96 and 0.04, respectively. The same deformed shape is noticed also as shown in Figure 3. The FEM gives good results close to previous experiments.

Table 1: FEM verification

Ref.	d_w (mm)	D_f (mm)	B_f (mm)	t_f (mm)	t_w (mm)	L (mm)	M_{EXP} (kN-m)	M_{FEM} (kN-m)	$\frac{M_{FEM}}{M_{EXP}}$
[15]	300	——	150	10	8	4600	124	113	0.91
	400	——	150	10	8	4600	158	153.51	0.97
	300	——	150	10	8	5600	102	109	0.93
[16]	100	25	75	2.5	3	1800	27.41	26.91	0.98
	100	25	75	1.6	3	1800	15.53	16.23	0.96
	200	25	75	1.3	1.6	1800	28.99	28.29	1.02

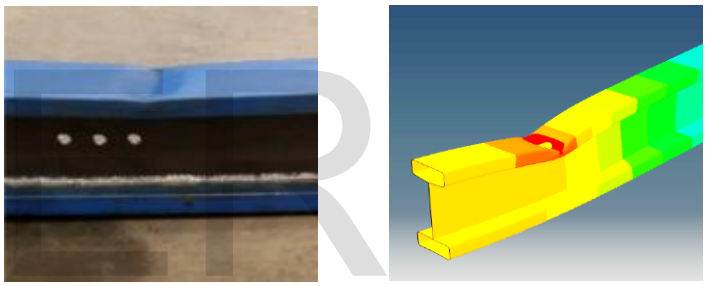

Fig.3: Deformation of experiment Ref [15] and current FEM

4 CURRENT STUDY

Different beams are modeled to investigate the moment capacity of HFB. The beam depth Df is taken constant as 1600 mm. The unsupported length L is taken 5, 10, 20, 30, 40, 50 & 60m. The hollow flange Bf x Df is taken 400 x 200 mm. The flange and web thickness are variable to cover wide range of slenderness ratio. The models cover compact, noncompact and slender flanges (CF, NF & SF), also compact, noncompact and slender web (CW, NW & SW).

4.1 Background on Moment Capacity in AISC

AISC360-16 provides equations to calculate the moment capacity of the common I beams. These equations are used for the current study on HFB. The design of beams as per AISC are controlled with three different failure modes: flange yielding (FY), compression flange local buckling (FLB), and overall lateral torsional buckling (LTB). The least value of nominal moment from these three different modes is calculated for each model and compared to the FEM result. The slenderness limits of compression parts of flange and web is calculated using the equations shown in Table 2. Also, the

limits of different lateral torsional buckling modes are calculated using the equations shown in the Table.

Table 2: AISC360-16 local buckling and lateral torsional buckling limits

Flange part subject to compression		Web part subject to bending	
$\lambda_{pf} = 1.12\sqrt{\frac{E}{F_y}}$	$\lambda_{rf} = 1.40\sqrt{\frac{E}{F_y}}$	$\lambda_{pw} = 3.76\sqrt{\frac{E}{F_y}}$	$\lambda_{rw} = 5.70\sqrt{\frac{E}{F_y}}$

		Limit of yielding	Limit of plastic LTB
CW	L_{pc} or L_{rc}	$1.76r_y\sqrt{E/F_y}$	$1.95r_t\frac{E}{0.7F_y}\sqrt{\frac{J}{S_xh_o}+\sqrt{\left(\frac{J}{S_xh_o}\right)^2+6.76\left(\frac{0.7F_y}{E}\right)^2}}$
NW	L_{pn} or L_{rn}	$1.1r_t\sqrt{E/F_y}$	
SW	L_{ps} or L_{rs}		$\pi r_t\sqrt{\frac{E}{0.7F_y}} = 3.755r_t\sqrt{\frac{E}{F_y}}$

Where:

λ_p = slenderness limit for compact case (f or w case of flange or web, respectively), λ_r = slenderness limit for noncompact case, E = modulus of elasticity, F_y = yield stress of steel, L_p = limits of lateral unbraced length for yielding (c or n or s case of compact or noncompact or slender web, respectively), L_r = limits of lateral unbraced length for plastic LTB, r_y = radius of gyration of section about minor axis, r_t = radius of gyration of compression flange + 1/3 of the compression web, S_x = elastic section modulus, ho = distance between the center of the two flanges, for tubular flange Ref. [8].

$$J = 2J_f + \frac{1}{3}d_w t_w^3 = 2x\frac{2\left((B_f - t_f)(D_f - t_f)\right)^2 t_f}{(B_f - t_f)+(D_f - t_f)} + \frac{1}{3}d_w t_w^3$$

4.2 Bahvior of HFB models

The relative lateral displacement between upper and lower flanges is extracted from each model. Sample of the relationship between normalized moment and relative lateral displacement is presented in Figure 4 for span 30 m. The curves of nine models are presented covering all classes of flange and web. Three groups of curves present the web class (CW, NW, and SW). Each group includes three curves representing the flange class (CF, NF, and SF). The curves show elastic behavior up to 40 to 50% the maximum moment then transferred to plastic behavior and ductile deformation. It is noticed that the curves of different flange classes are close which means the flange thickness has no effect on the moment capacity. On contrary, the web affects the moment capacity, as the models with smallest web thickness show low capacity compared to larger web thickness. The group of CW and NW shows moment capacity around 70% and 60% of yielding moment My, respectively. However, a deterioration in the capacity is found for SW where the capacity reach 30% of My.

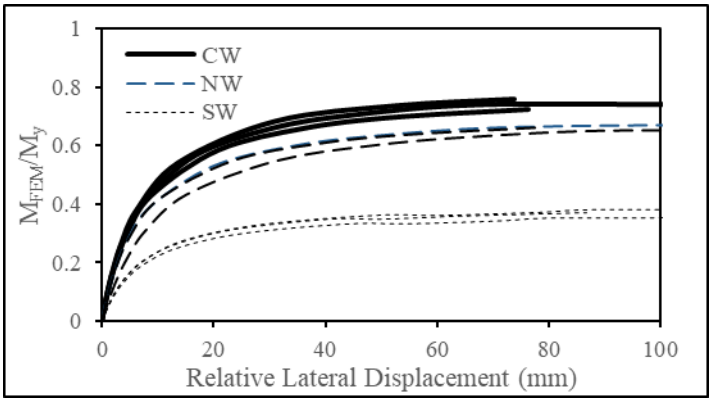

Fig.4 Normalized moment versus relative lateral displacement for HFB with L = 30 m

4.3 HFB with Compact Web

Reference to AISC, the moment capacity is a function of beam span. The relationship between moment and span starts with yielding then transition zone then ended with elastic lateral torsional buckling. In some cases of noncompact flange and for slender flange, flange local buckling governs the moment. The equation in AISC is presented as follows:

- Lateral Torsional Buckling (LTB)

$$M_n = M_p = Z_x F_y$$

→ For $L_b < L_{pc}$ (1)

$$M_n = C_b\left(M_p - (M_p - 0.7F_yS_x)\left(\frac{L_b - L_{pc}}{L_{rc} - L_{pc}}\right)\right)$$

→ For $L_{pc} < L_b \le L_{rc}$ (2)

$$M_n = C_b\left(\frac{\pi^2 E}{\left(\frac{L_b}{r_t}\right)^2}\sqrt{1 + 0.078\frac{J}{S_xh_o}\left(\frac{L_b}{r_t}\right)^2}\right)S_x$$

→ For $L_b > L_{rc}$ (3)

- Compression Flange Local Buckling (FLB)

$$M_n = M_p - (M_p - 0.7F_yS_x)\left(\frac{\lambda_f - \lambda_{pf}}{\lambda_{rf} - \lambda_{pf}}\right)$$

→ For $\lambda_{pf} < \lambda_f \le \lambda_{rf}$ (4)

$$M_n = \frac{0.9Ek_cS_x}{\lambda_f^2} \rightarrow \text{For } \lambda_f > \lambda_{rf} \quad (5)$$

Where:

Zx = plastic section modulus, Lb = lateral unsupported length of compression flange, Cb = LTB modification factor, λ_f = slenderness ratio of flange = Bf/tf or Df/tf for hollow flange,

IJSER

λw=slenderness ratio of web, $k_c = \frac{4}{\sqrt{h_c/t_w}} = \frac{4}{\sqrt{\lambda_w}} \geq 0.35 \;\&\; \leq 0.76$, hc = compression part of web.

The relationship between normalized moment and beam span for HFB with compact web is presented in three different curves as shown in Figures 5, 6 & 7 for CF, NF, and SF. FY controls the moment in very short spans while LTB controls the moment for medium to large spans. FLB takes place in short and medium spans for models with NF and in all spans for models with SF. This is the behavior reference to AISC equations while FEM shows different behavior. In CF, as shown in Figure 5, AISC is unconservative up to the elastic LTB at length around 40 m. Compared to LTB only, same behavior is noticed in Figure 6 & 7 for NF and SF, respectively. Regarding FLB, AISC equations give very low moment than FEM. The hollow flange of HFB is stiff and can resist local buckling because of its configuration as a tube, so the equations of FLB for common I shape with plated flange is not applicable on HFB.

As an adaptation of AISC for yielding zone, it is assumed that the plastic section modulus for HFB with CF shall not exceed 1.15 of the elastic section modulus, while this ratio is to be 1.00 in NF and SF. For long spans, it is assumed that LTB equations for both transition and elastic zones to be applied ignoring the FLB equations. As shown in Figures 5 to 7, the proposed equations that represented as continuous line are close and matching the FEM. The proposal can be applied to HFB.

As an adaptation of AISC for yielding zone, it is assumed that the plastic section modulus for HFB with CF shall not exceed 1.15 of the elastic section modulus, while this ratio is to be 1.00 in NF and SF. For long spans, it is assumed that LTB equations for both transition and elastic zones to be applied ignoring the FLB equations. As shown in Figures 5 to 7, the proposed equations that represented as continuous line are close and matching the FEM. The proposal can be applied to HFB.

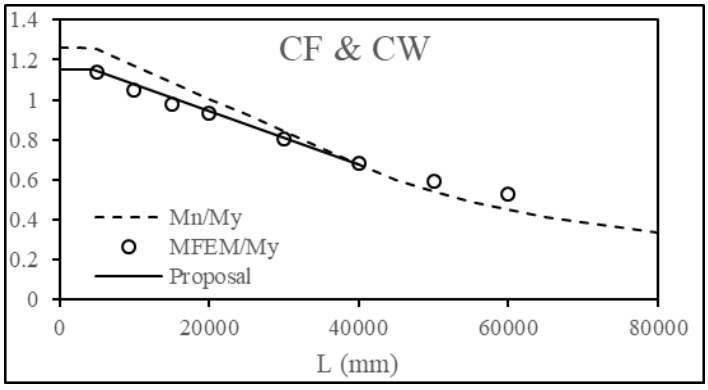

Fig.5. Normalized moment versus beam span relationship for HFB with CF and CW

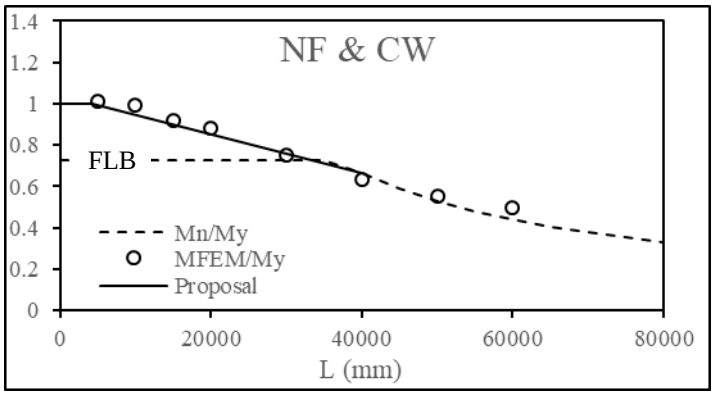

Fig.6. Normalized moment versus beam span relationship for HFB with NF and CW

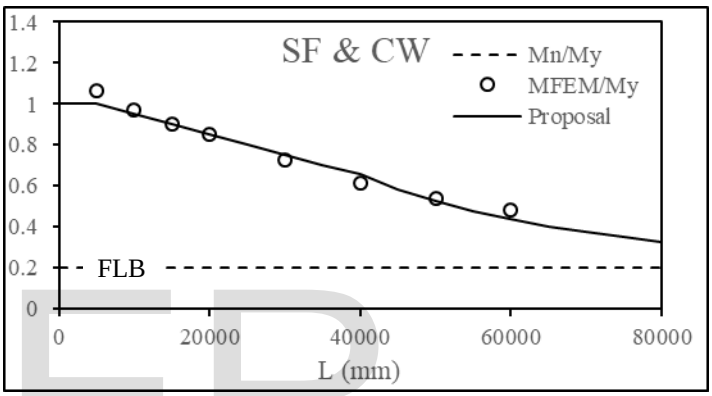

Fig.7. Normalized moment versus beam span relationship for HFB with SF and CW

4.3 HFB with Non-Compact Web

Same modes of failure for CW are applied on NW but with different equations. The AISC equations for NW are presented as follows:

- Lateral Torsional Buckling (LTB):

$$M_n = R_{pc}M_y = R_{pc}S_xF_y \rightarrow \text{For } L_b < L_{pn} \qquad (6)$$

$$M_n = C_b\left(R_{pc}M_y - (R_{pc}M_y - 0.7F_yS_x)\left(\frac{L_b - L_{pn}}{L_{rn} - L_{pn}}\right)\right)$$

$$\rightarrow \text{For } L_{pn} < L_b \leq L_{rn} \qquad (7)$$

$$M_n = C_b\left(\frac{\pi^2 E}{\left(\frac{L_b}{r_t}\right)^2}\sqrt{1 + 0.078\frac{J}{S_xh_o}\left(\frac{L_b}{r_t}\right)^2}\right)S_x$$

$$\rightarrow \text{For } L_b > L_{rn} \qquad (8)$$

IJSER

- Compression Flange Local Buckling (FLB):

$$M_n = R_{pc}M_y - (R_{pc}M_y - 0.7F_yS_x)\left(\frac{\lambda_f-\lambda_{pf}}{\lambda_{rf}-\lambda_{pf}}\right)$$

→ For $\lambda_{pf} < \lambda_f \le \lambda_{rf}$ (9)

$$M_n = \frac{0.9Ek_cS_x}{\lambda_f^2} \rightarrow \text{For } \lambda_f > \lambda_{rf} \quad (10)$$

Where:

Rpc = web plastification factor [$R_{pc} = 1.0$ For Iyc/Iy < 0.23, $R_{pc} = \frac{M_p}{M_y}$ For Iyc/Iy > 0.23 & λw < λpw, $R_{pc} = \left(\frac{M_p}{M_y} - \left(\frac{M_p}{M_y} - 1\right)\left(\frac{\lambda_w-\lambda_{pw}}{\lambda_r-\lambda_{pw}}\right)\right)$ For Iyc/Iy > 0.23 & λw > λpw, Iy = moment of inertia of section about minor axis, Iyc = moment of inertia of compression flange about minor axis.

The relationship between normalized moment and beam span for HFB with noncompact web is presented in Figure 8 in three different curves for CF, NF, and SF. Same trend as illustrated previously for CW is noticed. Reference to AISC, FY governs in very short spans with CF, LTB governs in medium and large spans with NC, FLB governs in short and medium spans with NF and in all spans with SF. FEM results did not follow AISC trend specially the FLB which is not applicable on HFB. For the LTB, AISC is found unconservative until the elastic LTB. Adaptation is assumed to the equation of elastic LTB by reducing the moment. A reduction factor for the term of the torsion constant is assumed function on LTB slenderness ratio. A new equation is proposed to replace Eq.8 for HFB with noncompact web as follows:

$$M_n = C_b\left(\frac{\pi^2E}{\left(\frac{L_b}{r_t}\right)^2}\sqrt{1 + 0.078\Omega_n\frac{J}{S_xh_o}\left(\frac{L_b}{r_t}\right)^2}\right)S_x$$

Where $\Omega_n = 3.3x10^{-3}\left(\frac{L_b}{r_t}\right) - 0.209$

As shown in Figure 8 the proposed equations that represented as continuous line are close and matching the FEM. The proposal can be applied to HFB with NW.

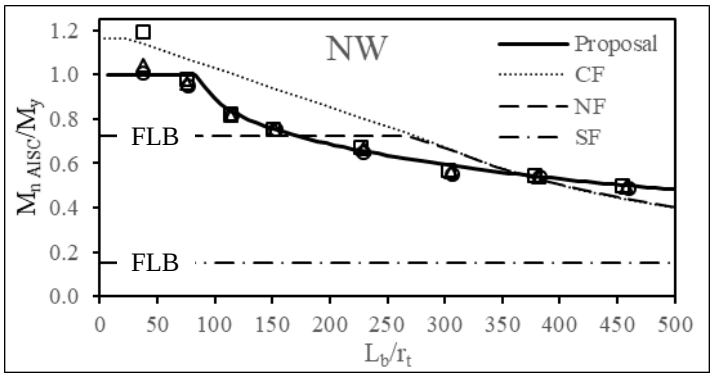

Fig. 8. Normalized moment versus LTB slenderness ratio relationship for HFB with NW

4.4 HFB with slender Web

The equations of AISC for models with slender web are presented below. The main difference is the elastic LTB where the torsion constant it totally neglected.

- Lateral Torsional Buckling (LTB):

$$M_n = R_{pg}M_y = R_{pg}S_xF_y \rightarrow \text{For } L_b < L_{ps} \quad (12)$$

$$M_n = C_b\left(R_{pg}M_y - 0.3R_{pg}M_y\left(\frac{L_b-L_{ps}}{L_{rs}-L_{ps}}\right)\right)$$

→ For $L_{ps} < L_b \le L_{rs}$ (13)

$$M_n = R_{pg}C_b\frac{\pi^2E}{\left(\frac{L_b}{r_t}\right)^2}S_x \rightarrow \text{For } L_b > L_{rs} \quad (14)$$

- Compression Flange Local Buckling (FLB)

$$M_n = R_{pg}M_y - 0.3R_{pg}M_y\left(\frac{\lambda_f-\lambda_{pf}}{\lambda_{rf}-\lambda_{pf}}\right)$$

→ For $\lambda_{pf} < \lambda_f \le \lambda_{rf}$ (15)

$$M_n = R_{pg}\frac{0.9Ek_cS_x}{\lambda_f^2} \rightarrow \text{For } \lambda_f > \lambda_{rf} \quad (16)$$

Where:

Rpg = bending strength reduction factor , aw = ratio of web area (twice compression part) to compression flange area , Afc = area of compression flange.

AISC trend of SW is similar to NW but with much lower nominal moment. The AISC equations are conservative with values much lower than FEM tends to zero up to only 12% of My. FEM shows moment around 40% of My in the long spans reach to 100% My in short spans. The reason is that AISC neglect torsion constant while it is effective in HFB due to the presence of the hollow flanges. An adaptation to AISC is proposed by return the torsion constant to the equation and add a reduction factor function on LTB slenderness ratio. A

new equation is proposed to replace Eq.14 for HFB with slender web as follows:

$$M_n = R_{pg}C_b\left(\frac{\pi^2E}{\left(\frac{L_b}{r_t}\right)^2}\sqrt{1 + 0.078\Omega_s\frac{J}{S_xh_o}\left(\frac{L_b}{r_t}\right)^2}\right)S_x$$

Where $\Omega_s = 2x10^{-6}\left(\frac{L_b}{r_t}\right)^2 - 2x10^{-4}\left(\frac{L_b}{r_t}\right) + 0.0633$

As shown in Figure 9 the proposed equations that represented as continuous line are close and matching the FEM. The proposal can be applied to HFB with SW.

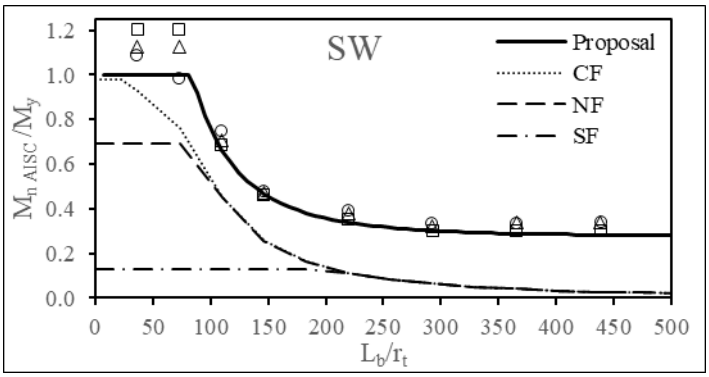

Fig. 9. Normalized moment versus LTB slenderness ratio relationship for HFB with SW

5 CONCLUSION

In summary, the following conclusion is driven from the current study. Hollow flange slenderness ratio has minor effect on the moment capacity of the HFB, while the web slenderness ratio has significant effect. Slender web reduces the moment capacity significantly. LTB equations available in AISC can be used to determine moment capacity of HFB in case of compact web after limiting the plastic moment to 1.15 of the yielding moment. For noncompact web, the LTB equations can be applied also after reducing the term of torsional rigidity. For slender web, neglecting torsion constant is not applicable for HFB. This term shall be added and reduction factor to be applied.

6 RECOMMENDATIONS

The following recommendations can be derived from the results and discussion provided in this paper:

- Investigate the impact of geometric configurations on various moment distributions.
- When determining the appropriate depth of web depth-to-plate width ratio, considers shear buckling.
- Examine the impact of web stiffeners on HFB sections created using the acceptable geometric parameters outlined in this study.

7 REFERENCES

[1] PI, Trahair, "Lateral distortional buckling of hollow flange beams", J. Struct. Eng. 123 (6), (1997) 695-702. DOI: 10.1061/(ASCE)0733-9445(1997)123:6(695)

[2] M. Mahendran, D. Mahaarachchi, "Section capacity tests of LiteSteel beam sections", Report No.2, Queensland Univ. of Technology (2005).

[3] T. Anapayan, M. Mahendran, D. Mahaarachchi, "Lateral distortional buckling tests of a new hollow flange channel beam", Thin-Walled Struct. 49 (1), (2011) 13-25. https://doi.org/10.1016/j.tws.2010.08.003

[4] A. Shaat, A. Matloub, A. Ibrahim, A. Dessouki, "Effect of web stiffeners on the lateral distortional buckling of channel section with hollow flanges", Ain Shams Eng. J. 13, (2022) 101517. https://doi.org/10.1016/j.asej.2021.06.003

[5] R. Sause, BG Kim, M. R. Wimer, "Experimental study of tubular flange beams", J. Struct. Eng. 134 (3), (2008) 384-392. http://dx.doi.org/10.1061/(ASCE)0733-9445(2008)134:3(384)

[6] J. Dong, R. Sause, "Moment strength of tubular flange beams", J. Constr. Steel Res. 65 (3), (2009) 622-630. https://doi.org/10.1016/j.jcsr.2008.02.019

[7] O. F. Kharoob, "Moment strength of steel plate beams with a tubular compression flange", ICE Proceedings Structures and Buildings 170 (3), (2017) 180-189. http://dx.doi.org/10.1680/jstbu.16.00176

[8] M. F. Hassanein, N. Silvestre, "Lateral-distortional buckling of hollow flange plate beams with slender unstiffened webs", Eng. Struct. 56, (2013) 572-584. http://dx.doi.org/10.1016/j.engstruct.2013.05.028

[9] M. F. Hassanein, O. F. Kharoob, A. M. ElHadidy, "Lateral-torsional buckling of hollow flange plate beams with slender stiffened webs", Thin-Walled Struct. 65, (2013) 49-61. http://dx.doi.org/10.1016/j.tws.2013.01.006

[10] M. F. Hassanein, O. F. Kharoob, "Moment strength of hollow flange plate beams with slender stiffened webs under mid-span concentrated loads", Thin-Walled Struct. 69, (2013) 18-28. http://dx.doi.org/10.1016/j.tws.2013.03.016

[11] M. F. Hassanein, O. F. Kharoob, "Shear strength and behavior of transversely stiffened tubular flange plate beams", Eng. Struct. 32, (2010) 2617-2630. doi:10.1016/j.engstruct.2010.04.034

[12] M. F. Hassanein, O. F. Kharoob, "An extended evaluation for the shear behavior of hollow flange plate beams", Thin-Walled Struct. 56, (2012) 88-102. http://dx.doi.org/10.1016/j.tws.2012.03.020

[13] ANSI/AISC 360-16, Specification for Structural Steel Buildings - American Institute of Steel Construction, (2016).

[14] ABAQUS Standard User's Manual, Hibbitt, Karlsson, and Sorensen. Inc. vol. 1, 2, and 3, version 6.4, USA, (2004).

[15] N. Perera, M. Mahendran, "Section moment capacity tests of hollow flange steel plate beams", J. Constr. Steel Res. 148, (2018) 97-111. https://doi.org/10.1016/j.jcsr.2018.04.034

[16] L. Kang. L. Meng, Y. Lin, "Experimental and numerical investigation of lateral torsional buckling behavior and capacity of welded Q460 beams", J. Constr. Steel Res. 172, (2020) 106166. https://doi.org/10.1016/j.jcsr.2020.106166

IJSER